Journal of Power Sources 307 (2016) 86–97

Contents lists available at ScienceDirect

Journal of Power Sources

journal homepage: www.elsevier.com/locate/jpowsour

Electrochemical model parameter identification of a lithium-ion battery using particle swarm optimization method

Md Ashiqur Rahman [a], Sohel Anwar [a, *], Afshin Izadian [b]

[a] Department of Mechanical Engineering, Purdue School of Engineering and Technology, IUPUI, Indianapolis, IN 46202, USA
[b] Energy Systems and Power Electronics Lab, Purdue School of Engineering and Technology, IUPUI, Indianapolis, IN 46202, USA

HIGHLIGHTS

- Four critical electrochemical model parameters of a Li-Ion battery were identified.
- A cost function was defined to minimize voltage error between model and test data.
- Particle swarm optimization methodology was utilized to minimize the cost function.
- Four sets of these critical model parameters were identified for the stated conditions.

ARTICLE INFO

Article history:
Received 20 July 2015
Received in revised form
13 December 2015
Accepted 17 December 2015
Available online xxx

Keywords:
Electrochemical model
Lithium-ion batteries
Particle swarm optimization
Parameter identification
Battery management system

ABSTRACT

In this paper, a gradient-free optimization technique, namely particle swarm optimization (PSO) algorithm, is utilized to identify specific parameters of the electrochemical model of a Lithium-Ion battery with $LiCoO_2$ cathode chemistry. Battery electrochemical model parameters are subject to change under severe or abusive operating conditions resulting in, for example, over-discharged battery, over-charged battery, etc. It is important for a battery management system to have these parameter changes fully captured in a bank of battery models that can be used to monitor battery conditions in real time. Here the PSO methodology has been successfully applied to identify four electrochemical model parameters that exhibit significant variations under severe operating conditions: solid phase diffusion coefficient at the positive electrode (cathode), solid phase diffusion coefficient at the negative electrode (anode), intercalation/de-intercalation reaction rate at the cathode, and intercalation/de-intercalation reaction rate at the anode. The identified model parameters were used to generate the respective battery models for both healthy and degraded batteries. These models were then validated by comparing the model output voltage with the experimental output voltage for the stated operating conditions. The identified Li-Ion battery electrochemical model parameters are within reasonable accuracy as evidenced by the experimental validation results.

1. Introduction

Amongst all the alternative energy sources available for various propulsion applications such as plug-in hybrid electric vehicle (PHEV), hybrid electric vehicle (HEV), and electric vehicle (EV), Lithium-Ion (Li-ion) battery is considered to be the most promising [1]. Compared to the other alternative options for energy sources (such as Nickel–Cadmium, Nickel-Metal Hydride, etc.), Lithium-Ion batteries have some unique advantages such as higher specific energy, minimum memory effect, best energy-to-weight ratio, and low self-discharge when idle [2,3]. Based on these stated advantages, Li-Ion batteries are the leading candidate for the upcoming generation of automotive, aerospace, and other applications.

PHEV, HEV, and EV have been gaining more acceptance in recent years due to their lower emission rates and better fuel efficiency [4]. Performance of these transportation options are significantly dependent on the electrochemical energy sources, e.g. installed battery modules integrated with the vehicle powertrain. Depending on the user driving habits and the road conditions, these traction batteries undergo different operating conditions as the battery load demand changes. The safe operation of the entire battery

* Corresponding author.
E-mail addresses: rahman2@iupui.edu (M.A. Rahman), soanwar@iupui.edu (S. Anwar), aizadian@iupui.edu (A. Izadian).

http://dx.doi.org/10.1016/j.jpowsour.2015.12.083
0378-7753/

Nomenclature

c_e	lithium ion concentration in the electrolyte phase	n	number of active materials
c_s	lithium ion concentration in the active materials in both electrodes	R	universal gas constant
		R_p	radius of the spherical particles
$\bar{c}_{s,i}$	volume-averaged concentration of a single particle	t_c^0	transference number
D_e	diffusivity at electrolyte phase	T	average internal temperature
D_s	diffusivity at solid phase	U	open circuit potential
$f_{\pm a}$	mean molar activity coefficient	V	cell voltage
F	Faraday constant	α_a	charge transfer coefficient in anode
i_e	current in the electrolyte phase	α_c	charge transfer coefficient in cathode
i_0	exchange current density	γ	observer gain constant
I	load current	ϕ_e	potential at electrolyte phase
j_n	molar ion fluxes between the active materials in electrodes and the electrolyte	ϕ_s	potential at solid phase
		ε_e	volume fraction at electrolyte phase
		ε_s	volume fraction at solid phase
L^-	length of negative electrode	η	over-potential for the reactions
L^+	length of positive electrode	ρ^{avg}	average density
		κ	intercalation/de-intercalation reaction rate

module is always expected, as it is one of the most vital components of the stated vehicle configurations. But in reality, it is not always possible to maintain the desired safe and healthy operating conditions of the battery system for a number of reasons. For instance, battery can be overcharged during operation, or over-discharged at different rates. Moreover, battery degradation due to aging is another potential situation arising out of long-term cycling of the battery.

In HEVs, the onboard battery management system (BMS) is responsible for managing the rechargeable battery system by monitoring its state of charge (SOC), protecting the battery from unsafe operating zones, and reporting the diagnostic data to the operator while managing the battery operation. An accurate monitoring of the battery state is possible if the critical battery parameters can be reliably identified which can consequently lead to a better BMS. With this objective, identification of four critical battery parameters of an electrochemical battery model with $LiCoO_2$ cathode chemistry is developed in this work. It is to be noted that a $LiCoO_2$ cathode based Li-Ion battery offers high energy density compared to other Li-Ion battery chemistries such as $LiFePO_4$ cathode. Also, the electrochemical model of a Li-Ion battery captures a more realistic chemical kinetics and electro-dynamics in a cell compared to other modeling methodologies such as equivalent circuit model. Amongst all the parameters of the electrochemical model of Li-Ion battery, the principal reason for selecting these four parameters (e.g. solid phase diffusion coefficient at the cathode, solid phase diffusion coefficient at the anode, intercalation/de-intercalation reaction rate at the cathode, and intercalation/de-intercalation reaction rate at the anode) is that these parameters exhibit significant variations when the battery is subject to severe or abusive conditions such as overcharging, over-discharging, adverse environmental conditions, etc. [13].

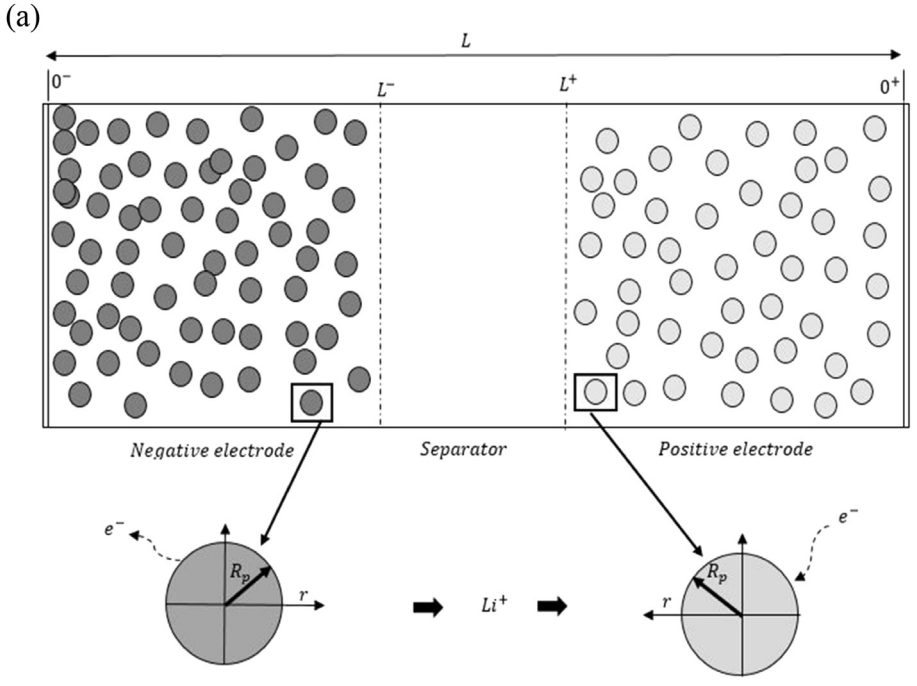

Fig. 1. (a) Schematic of Li-Ion battery geometry; (b) PSO algorithm flowchart.

(b)

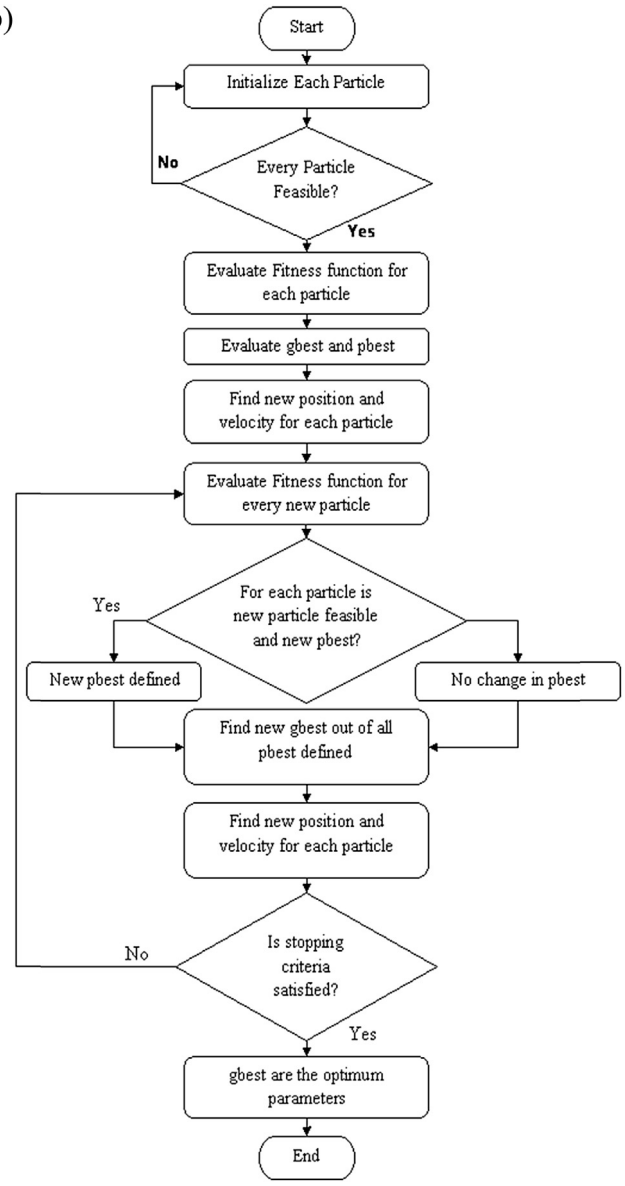

Fig. 1. (*continued*).

An accurate identification of the critical model parameters of the battery can lead to a better battery management system through better condition monitoring and fault diagnosis of the battery. Particle Swarm Optimization (PSO) is a non-gradient based optimization method that was originally developed by Kennedy and Eberhart in 1995 [5,6]. The stated battery electrochemical parameters can be identified with high accuracy through the optimization of an appropriate fitness function. The identified parameters can be used to generate different battery model simulating various battery characteristics based on the operating conditions. Such battery models can be used to develop robust fault diagnosis algorithms.

"Evolutionary Algorithms" are a population based heuristic approach for optimization of a cost function which is gradient free. Particle Swarm optimization (PSO) algorithm is one of the methodologies classified as evolutionary algorithm. Chakraborti et al. [7,8] utilized evolutionary algorithms to optimally design the negative electrode of a Li-Ion battery where the performance of PSO algorithm was found to be superior. However, most of the studies in parameter identification of a Li-Ion battery electrochemical model predominantly utilized genetic algorithm (GA) based methods [9–11]. Amongst all evolutionary algorithms, PSO offers distinct notable advantages such as utilization of two populations which allow greater diversity and exploration over a single population as in genetic algorithm. In addition, the momentum effects on particle movement can allow faster convergence and more variety/diversity in search trajectories. PSO does not involve the mutation and crossover function.

Although particle swarm optimization algorithm has been used in parameter identification [12], identification of the electrochemical model parameters of a Li-Ion battery has not been reported in literature. Parameter estimation of the physics based or the electrochemical model of Li-Ion battery were carried out in Refs. [13,14]. Ramadesigan et al. [13] demonstrated that capacity fade in a Li-Ion battery with $LiMnO_2$ cathode results into significant variation in the solid-phase diffusion coefficient and the reaction rate constant of the electrochemical model. They used Gauss-Newton method to estimate the model parameters. Subramanian et al. [14] provided a fast simulation method for physics based lithium-ion battery models. Speltino et al. [15] presented experimental validation of Li-Ion battery electrochemical model with the identified parameter. However, the paper does not indicate whether it has used PSO algorithm except that it used a MATLAB based gradient free function minimization algorithm. Moreover, it did not identify the reaction rate constants for the electrochemical model. Li-Ion battery electrochemical model proposed by Doyle et al. [16,17] is a physics-based model that contains the required information to capture the battery electrochemistry. Hence it is more realistic than other available models. PSO based parameter identification for Li-Ion battery model can offer an improved convergence on the battery electrochemical model parameters, particular those that are subject to noticeable variations under severe or abusive operating conditions resulting in capacity fade.

In this work, identification of the stated parameters and the validation of the reduced order electrochemical Li-Ion battery model were performed by comparing the model output voltage with the experimentally measured voltage. The experiments were carried out on Panasonic NCR18650B 3.4 A h, 3.7 V Li-Ion batteries with $LiCoO_2$ cathode by a battery tester (Model: CADEX C8000) in the Mechatronics Research Laboratory, IUPUI. The batteries were conditioned to attain different states they might operate in, e.g. Navy over-discharge cycle, over-charge cycle, etc. along with the normal operating condition of the battery. The battery model parameters for each of these cases were identified using the PSO algorithm.

This paper is organized as follows. The next section illustrates the battery electrochemical model used in this work. It is followed by the presentation of the reduced order Li-ion electrochemical battery model. Section 4 provides a brief summary of particle swarm optimization (PSO) method which is followed by the parameter identification of battery electrochemical model parameters in Section 5. Experimental results are presented in Section 6–7 which is followed by the discussion of the model validation using experimental and simulated data. Lastly the findings of this work are summarized in the conclusion section.

2. Electrochemical battery model

The electrochemical battery model captures the spatiotemporal dynamics of Li-Ion concentration, electrode potential in each phase, and the Butler-Volmer kinetics which governs the intercalation reactions [16]. A schematic of the model is provided in Fig. 1(a) [18].

In the provided geometry, the model considers the dynamics of Li-ion cell only in X-direction. Therefore, the model considered in this work is a 1-D spatial model where variations of the dynamics in

Y and Z directions are assumed to be small. It is also assumed that Li-ion particles are considered to be of spherical shapes with mean radius of R_p situated along X-axis [19].

In Fig. 1(a), the main regions of the Li-ion battery model are shown. The entire spatial length is divided into three regions, namely, negative electrode (ranges from 0^- to L^-), separator (ranges from L^- to L^+), and the positive electrode (ranges from L^+ to 0^+). Two electrodes are separated by the thin and porous separator region through which only lithium ions (Li^+) can pass, i.e. the electrons must flow through the circuit outside the battery [19].

The state variables of the full battery model at any instantaneous time, t, and distance, x, are lithium ion concentration in the electrolyte phase, lithium ion concentration in the active materials in both electrodes, potential at electrolyte phase, potential at solid states, current in the electrolyte phase, molar ion fluxes between the active materials in electrodes and the electrolyte and the average internal temperature [1].

The governing equations of the electrochemical model of the Li-ion battery are given by the following set of partial differential algebraic equations (PDAE) [1,3,16,17,19–21]:

$$\varepsilon_e \frac{\partial c_e(x,t)}{\partial t} = \frac{\partial}{\partial x}\left(\varepsilon_e D_e \frac{\partial c_e(x,t)}{\partial x} + \frac{1-t_c{}^0}{F} i_e(x,t)\right) \tag{1}$$

$$\frac{\partial c_{s,i}(x,r,t)}{\partial t} = \frac{1}{r^2}\frac{\partial}{\partial r}\left(D_{s,i} r^2 \frac{\partial c_{s,i}(x,r,t)}{\partial r}\right) \tag{2}$$

a constant.

The cell temperature is considered to be lumped and was modeled based on the following equation [1]:

$$\rho^{avg} c_p \frac{dT(t)}{dt} = h_{cell}(T_{amb} - T(t)) + I(t)V(t) - \sum_{i=1}^{i=n}\left[\int_{0^-}^{0^+} \frac{3\varepsilon_{s,i}}{R_{p,i}} F j_{n,i}(x,t) \Delta U_i(x,t) dx\right] \tag{9}$$

Where,

$$\Delta U_i(x,t) \triangleq U_i(\bar{c}_{s,i}(x,t)) - T(t)\frac{\partial U_i(\bar{c}_{s,i}(x,t))}{\partial T} \tag{10}$$

Here, $\bar{c}_{s,i}(x,t)$ is the volume-averaged concentration of a single particle, which is again defined as:

$$\bar{c}_{s,i}(x,t) \triangleq \frac{3}{R_{p,i}^3}\int_0^{R_{p,i}} r^2 c_{s,i}(x,r,t) dr \tag{11}$$

In the above equations ε_e, $\varepsilon_{s,i}$, σ, R, $R_{p,i}$, F, α_a, α_c, c_p, ρ^{avg}, h_{cell} and t_c^0 are all constant parameters while κ, $f_{c/a}$ and D_e are dependent on electrolyte concentration and temperature and $r_{eff,i}$, $D_{s,i}$ and R_f are Arrhenius-like parameters which follows the equation [1]:

$$\theta(T) = \theta_{T_0} e^{A_\theta((T(t)-T_0)\div(T(t)T_0))} \tag{12}$$

The open circuit potential for the positive electrode (cathode) is given by the following empirical equation [22]:

$$U_p = \frac{-4.656 + 88.669\theta_p^2 - 401.119\theta_p^4 + 342.909\theta_p^6 - 462.471\theta_p^8 + 433.434\theta_p^{10}}{-1 + 18.933\theta_p^2 - 79.532\theta_p^4 + 37.311\theta_p^6 - 73.083\theta_p^8 + 95.96\theta_p^{10}} \tag{13}$$

$$\frac{\partial \phi_e(x,t)}{\partial x} = -\frac{i_e(x,t)}{\kappa} + \frac{2RT}{F}\left(1-t_c{}^0\right)\left(1 + \frac{d\ln f_{c/a}}{d\ln c_e(x,t)}\right)\frac{\partial c_e(x,t)}{\partial x} \tag{3}$$

$$\frac{\partial \phi_s(x,t)}{\partial x} = \frac{i_e(x,t) - I(t)}{\sigma} \tag{4}$$

$$\frac{\partial i_e(x,t)}{\partial x} = \sum_{i=1}^{i=n} \frac{3\varepsilon_{s,i}}{R_{p,i}} F j_{n,i}(x,t) \tag{5}$$

$$j_{n,i}(x,t) = \frac{i_{0,i}(x,t)}{F}\left(e^{\frac{\alpha_a F \eta_i(x,t)}{RT}} - e^{\frac{-\alpha_C F \eta_i(x,t)}{RT}}\right) \tag{6}$$

Here $i_{0,i}(x,t)$ is the exchange current density and $\eta_i(x,t)$ is the over-potential for the reactions, equations of which are [1]:

$$i_{0,i}(x,t) = r_{eff,i} c_e(x,t)^{\alpha_a}\left(c_{s,i}^{\max} - c_{ss,i}(x,t)\right)^{\alpha_c} c_{ss,i}(x,t)^{\alpha_C} \tag{7}$$

$$\eta_i(x,t) = \phi_s(x,t) - \phi_e(x,t) - U(c_{ss,i}(x,t)) - FR_{f,i} j_{n,i}(x,t) \tag{8}$$

Here, $c_{ss,i}(x,t)$ is the i^{th} concentration at solid phase evaluated at $r = R_{p,i}$,$U(c_{ss,i}(x,t))$ is the open circuit potential of the i^{th} active material in the solid phase and $c_{s,i}^{\max}$ is the maximum possible concentration in the solid phase of the i^{th} active material and this is

Where, $\theta_p = c_{s,p}/c_{s,p,\max}$ is a dimensionless number ranges from 0 to 1.

Similarly, the open circuit potential for the negative electrode (anode) is given by Ref. [22]:

$$U_n = 0.7222 + 0.1387\theta_n + 0.029\theta_n^{0.5} - \frac{0.0172}{\theta_n} + \frac{0.0019}{\theta_n^{1.5}} + 0.2808\exp(0.9 - 15\theta_n) - 0.7984\exp(0.4465\theta_n - 0.4108) \tag{14}$$

Where, $\theta_p = c_{s,n}/c_{s,n,\max}$ is also a dimensionless number ranges from 0 to 1.

Output voltage of the battery model is then given by Ref. [1],

$$V(t) = \phi_s\left(0^+,t\right) - \phi_s\left(0^-,t\right) \tag{15}$$

3. Model reduction

Due to the complexity of the stated PDAE model, the electrochemical model is reduced based on a few simplifying assumptions [1]. The intention of reduction is to build a model from the simulation point of view while maintaining the ability to capture all the

cell dynamics [1]. The key assumption made here is that the electrolyte concentration is constant, i.e. $c_e(x,t) = c_e$ [1]. Another assumption is the introduction of an approximate solution of the diffusion equations in the solid active materials in each electrode as presented in Ref. [23]. Using these two assumptions, the reduced order PDAE equations can be presented as follows [1]:

$$\frac{\partial}{\partial t}\bar{c}_{s,i}{}^{\pm}(x,t) = -\frac{3}{R_i^{\pm}} j_{n,i}{}^{\pm}(x,t) \tag{16}$$

$$\frac{\partial}{\partial t}\bar{q}_{s,i}{}^{\pm}(x,t) = -\frac{30}{\left(R_i^{\pm}\right)^2}\bar{q}_{s,i}{}^{\pm}(x,t) - \frac{45}{2\left(R_i^{\pm}\right)^2} j_{n,i}{}^{\pm}(x,t) \tag{17}$$

$$c_{ss,i}{}^{\pm}(x,t) = \bar{c}_{s,i}{}^{\pm}(x,t) + \frac{8R_i^{\pm}}{35}\bar{q}_{s,i}{}^{\pm}(x,t) - \frac{R_i^{\pm}}{35D_{s,i}{}^{\pm}} j_{n,i}{}^{\pm}(x,t) \tag{18}$$

$$j_{n,i}{}^{\pm}(x,t) = \frac{i_{0,i}{}^{\pm}(x,t)}{F}\left(e^{\frac{\alpha_a F \eta_i{}^{\pm}(x,t)}{RT}} - e^{\frac{-\alpha_C F \eta_i{}^{\pm}(x,t)}{RT}}\right) \tag{19}$$

$$\frac{\partial i_e{}^{\pm}(x,t)}{\partial x} = \sum_{i=1}^{i=n} \frac{3\varepsilon_{s,i}{}^{\pm}}{R_{p,i}{}^{\pm}} F j_{n,i}{}^{\pm}(x,t) \tag{20}$$

$$\frac{\partial \phi_s{}^{\pm}(x,t)}{\partial x} = \frac{i_e{}^{\pm}(x,t) - I(t)}{\sigma^{\pm}} \tag{21}$$

$$\frac{\partial \phi_e{}^{\pm}(x,t)}{\partial x} = -\frac{i_e{}^{\pm}(x,t)}{\kappa} \tag{22}$$

$$\begin{aligned}\rho^{avg} c_p \frac{dT(t)}{dt} = {} & h_{cell}(T_{amb} - T(t)) + I(t)V(t) \\ & - \sum_{i=1}^{i=n}\left[\int_{0^-}^{L^-} \frac{3\varepsilon_{s,i}{}^{-}}{R_{p,i}{}^{-}} F j_{n,i}{}^{-}(x,t)\Delta U_i{}^{-}(x,t)dx\right] \\ & - \sum_{i=1}^{i=n}\left[\int_{0^+}^{L^+} \frac{3\varepsilon_{s,i}{}^{+}}{R_{p,i}{}^{+}} F j_{n,i}{}^{+}(x,t)\Delta U_i{}^{+}(x,t)dx\right]\end{aligned} \tag{23}$$

Boundary conditions for the above reduced order model are given by:

$$\phi_e{}^{+}\left(0^+,t\right) = 0,\ \phi_e{}^{-}\left(L^-,t\right) = \phi_e{}^{+}\left(L^+,t\right) - \frac{I(t)L^{sep}}{\kappa^{sep}}$$

$i_e{}^{\pm}(0^{\pm},t) = 0$ and $i_e{}^{\pm}(L^{\pm},t) = \pm I(t)$

The initial conditions of this model are:

$c_{s,i}{}^{\pm}(x,0) = \bar{c}_{s,i,0}{}^{\pm}(x)$, $\bar{q}_{s,i}{}^{\pm}(x,0) = \bar{q}_{s,i,0}{}^{\pm}(x)$ and $T(0) = T_0$

The voltage output equation for this reduced order model remains the same as previously mentioned, i.e.

$$V(t) = \phi_s\left(0^+,t\right) - \phi_s\left(0^-,t\right) \tag{24}$$

4. Particle swarm optimization (PSO) algorithm

The PSO algorithm has some similarity with other heuristic search techniques, e.g. genetic algorithm (GA) [5]. Like GA, PSO is also initialized with some population of random candidates [5,12,24–29] and a search algorithm to reach the global minimum for the defined objective or fitness function. This is accomplished by updating the generations from iteration to iterations. There are clear differences between GA and PSO in terms of simulation time. PSO instead of using mutation and crossover has particles or the potential candidate solutions that move randomly through the problem space and search for the global optimum value [30], which requires less time as compared with GA. In PSO, each of the particles keeps the record of the particular best location (coordinate in the problem space) which gives the best value of the fitness function with respect to that particle. This position/location value is denoted by particle best value or **pbest** [28]. After gathering the information of **pbest** for each particle, the algorithm uses these values to find the global optimal solution which is denoted by **gbest** [28].

In each iteration of PSO, particle velocity is updated which is associated with random numbers. According to these velocity updates, particle positions are also updated [30]. These updated positions and the velocities values are used to find the optimal solution.

The equations with which the velocity and the positions of the particles are updated, are given by Ref. [28]:

$$v_i^{k+1} = w v_i^k + c_1 r_i^k\left(p_i^k - x_i^k\right) + c_2 s_i^k\left(g_i^k - x_i^k\right) \tag{25}$$

$$x_i^{k+1} = x_i^k + v_i^{k+1} \tag{26}$$

Where, r and s are random numbers.

In this algorithm, w is referred as the inertia constant and its recommended value is slightly less than 1, usually from 0.7 to 0.8, c_1 and c_2 are the constants, which determine how much the particles are directed towards an ideal position. One of them is termed as cognitive component and the other one is designated as social component. The significance of these two constants is that, they determine how much the particle best position and the global best position value affect the particles movement. Recommended value for these two constant is approximately 2 [31]. A flowchart representing the PSO algorithm is provided in Fig. 1(b). In this work, the optimality condition was checked by observing the convergence of the fitness function. Similar convergence was reported in Ref. [33] where a PSO problem with constraints was simulated and the optimality was checked using Karush-Kuhn-Tucker (KKT) error based stopping criteria. The convergence pattern in this paper closely resembles closely the convergence pattern presented here, providing additional support of validity of the optimized cost function.

5. Parameter identification

Although the electrochemical model of Li-Ion battery in Section 3 is of reduced order, it still depends on a significant number of parameters. Of these parameters, some are dependent on the geometry of the battery, which can be regarded as the physical parameters while other parameters are dependent on the chemistry of the battery. In this study, a number of the parameter values are adopted from literature while a number of other parameter values are obtained from the battery manufacturer's specification.

The general parameter values for the stated battery models are adopted from Ref. [22] for the simulation of the reduced electrochemical model (excluding the ones responsible for battery state change) and are given in Table 1.

However, four major parameters that have been reported to exhibit significant variation [13] depending on battery operating conditions (e.g. severe or abusive charge/discharge cycling) are the subject of the parameter identification work presented here. The parameters to be identified in this work are: solid phase diffusion

Table 1
Electrochemical model parameters for $LiCoO_2$ cathode chemistry.

Symbol	Unit	Cathode	Separator	Anode
σ_i	S/m	100		100
$\varepsilon_{f,i}$		0.025		0.0326
ε_i		0.385	0.724	0.485
$c_{s,i,max}$	mol/m^3	51554		30555
$c_{s,i,0}$	mol/m^3	0.4955 × 51554		0.8551 × 30555
c_0	mol/m^3		1000	
R_p	m	2×10^{-6}		2×10^{-6}
L_i	m	80×10^{-6}	25×10^{-6}	88×10^{-6}
R_{SEI}	Ωm^2	0	0	0
F	C/mol	96487	96487	96487
R	J/(mol K)	8.314	8.314	8.314
T	K	298.15	298.15	298.15

coefficient at positive electrode (cathode), solid phase diffusion coefficient at the negative electrode (anode), intercalation/de-intercalation reaction rate at cathode and intercalation/de-intercalation reaction rate at anode. The principal reason for selecting these four parameters is that, these parameters exhibit significant variations when the battery is subject to abusive conditions such as overcharging, over-discharging and adverse environmental conditions etc. [13].

For the identification of battery electrochemical parameters via particle swarm optimization, all the selected parameters need be initialized. The initial values of the parameters to be identified were assumed based on the values found in literature [32] for $LiCoO_2$ cathode chemistry which are provided in Table 2. These battery parameter values were used in initializing the particle swarm optimization (PSO) algorithm.

The objective or fitness function for the proposed parameter identification method via PSO algorithm is defined by the following function [15]:

$$\min \int_{t=1}^{t=n} (V_e - V_m)^2 dt$$

Here, V_m is the predicted model output voltage corresponding to an input current signal, V_e is the measured experimental output voltage corresponding to the same input current, t is the time, and n is number of samples in the current signal.

There is a preset maximum allowable limit of the defined error function or the objective function, under which the fitness function can be regarded as having reached the optimal value. Consequently the corresponding parameter values are considered to have been identified since the objective function is minimized for that particular condition of the battery. In this parameter identification work, this limit was set at 0.5, which is based on fitness function convergence characteristics. The optimization algorithm runs until the fitness function reaches the optimal value. Cost function evaluation technique using PSO for constrained optimization problem is illustrated in Ref. [33]. The methodology of the cost function evaluation in this reference is similar to the work presented here.

In this work, the number of particles for each of the target parameters were chosen to be three (3). The learning parameter values in this algorithm were taken as $c_1 = 2$ and $c_2 = 1$, while the inertia factor was chosen to be $w = 0.5$.

Table 2
Initial values of the parameters to be identified.

Parameter to be identified	Initial maximum value
$D_{s,p}$	1×10^{-15}
$D_{s,n}$	2×10^{-16}
κ_p	3×10^{-14}
κ_n	5×10^{-16}

6. Experimental results

The experimental setup for this parameter identification work is shown in Fig. 2. Batteries were tested using CADEX C8000 battery tester and the experimental results were continuously monitored for the identification purpose.

For parameter identification, the battery states under consideration were obtained via experimentations using the following charge/discharge regimes:

1. Healthy battery charge–discharge regime: The Li-Ion battery is discharged at a nominal rate of 1 C to a low SOC level (below 10%). This is followed by a nominal (1 C) charging of the battery to a fully charged state. This cycle is repeated 20 times and the critical battery parameters are monitored.
2. Navy over-discharged cycle: The Li-ion battery is discharged at maximum suitable discharge rate of 25% over discharge (1.25 C). The charging of the battery is carried out using a standard non-abusive charge regime (1 C). The battery is cycled 20 times using this discharge-charge regime and the critical battery parameters are monitored.
3. 24-hr over-discharged cycle: The Li-Ion battery is discharged at a suitable discharge rate (1.2 C) until the SOC reaches zero. To maintain near zero terminal voltage, a resistor is connected across the terminals for the duration of 24 h. The charging of the battery is then carried out using a standard non-abusive charging profile (1 C). The 24 h over discharge test cycle is repeated 20 times and the battery parameters are monitored.
4. Overcharged battery cycle: The Li-Ion battery is discharged at a nominal discharge rate (1 C) to a low SOC level (below 10%). This is followed by a 25% over-charge (1.25 C) of the battery. This cycles is repeated 20 times and the critical battery parameters are monitored.

6.1. Healthy battery parameter identification

The healthy operation of the battery was carried out as described above. The battery was discharged at 3.4 A and the charge regime was also run at 3.4 A. This healthy operating cycle was continued for twenty (20) cycles. The experimental output voltage for the last cycle (for both discharge and charge regimes) was recorded and the fitness function was computed using the simulated output voltage of the battery electrochemical model. The trajectory of the particles for each of the four stated parameters was monitored to ensure the particle convergence as required by the PSO algorithm. The global best particle history was also monitored to check the optimum value of the fitness function.

PSO algorithm's convergence is dependent on the selection of initial particle position. It is often necessary to try a number of initial particle positions before settling on the appropriate initial positions of the particles. Here, the initial particle positions were selected after trying a number of positions. The particle update histories by PSO algorithm for all of the parameters mentioned in the previous section for healthy battery charging operation are provided in Fig. 3(a)-(d). From the particle position update history for each iteration, it is clear that the particles converged to a single location from their initial positions, which is required by the PSO algorithm. While observing the particles' trajectories' convergence, the global minimum value of the fitness function was obtained and is shown in Fig. 3(e). The optimized fitness function established

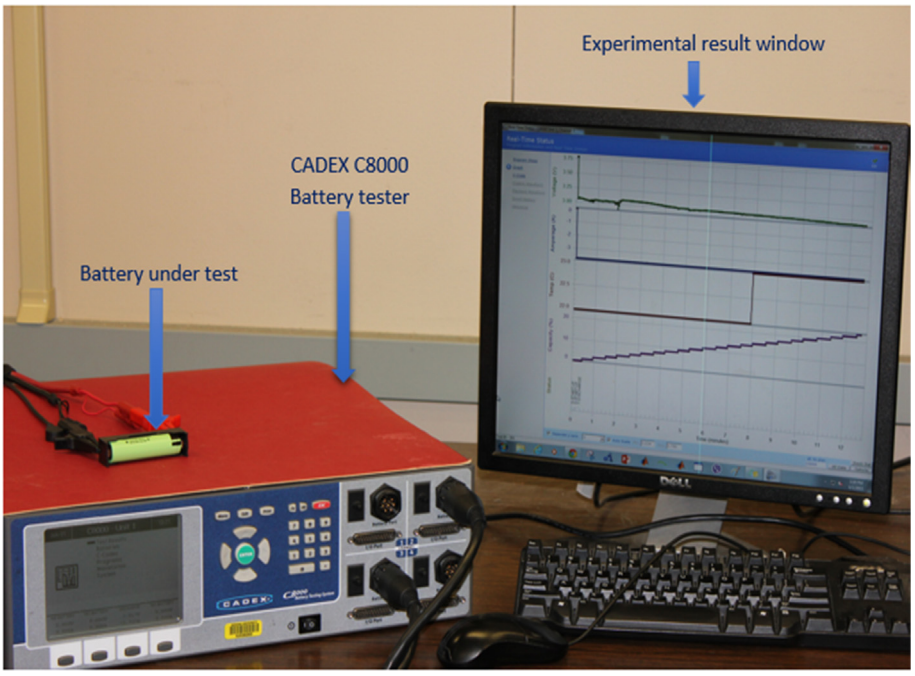

Fig. 2. Experimental setup for battery testing.

through the convergence essentially provides the estimate of the target parameters of the battery electrochemical model.

The parameters were identified for both discharging and charging part of the last cycle of operation for the healthy battery. The identified values of the parameters and the corresponding fitness function values are provided in Table 3.

6.2. Navy over-discharged battery parameter identification

In this parameter identification scenario the discharge operation was carried out at 4.25 A current (25% over-discharge) and the charging operation was performed at 3.4 A (1 C charging). This pattern of operation was repeated for twenty (20) cycles and the identification was carried out for the last cycle of operation. This cycling ensured that the battery state was reduced to an over-discharged condition. The particles' trajectory of the parameters is provided in Fig. 4(a)-(d). For this over-discharged battery, the discharge operation is more significant as compared with the charge operation. Therefore, the discharge regime parameter particle trajectories are provided for the corresponding discharge current although the parameters were identified for both discharge and charge regions.

From Fig. 4, it is clear that the parameter particles for each parameter converged to a single location as for the over-discharged battery parameters' trajectories. The fitness function was observed throughout the iterations for the identification process. The trajectory for the fitness function is provided in Fig. 4(e). The identified parameters for both discharge and charge regions for the Navy over-discharged battery are provided in Table 4.

6.3. 24-hr Over-discharged battery parameter identification

In this parameter identification scenario, the battery was discharged at 4.08 A (20% over-discharge) and then charged at 3.4 A (1 C). Under this operating condition, the battery was discharged at the stated rate, until the battery SOC (capacity of the battery) reached zero. It was then following by charging at normal 1 C rate. This pattern of operation was repeated for twenty (20) times and the last region was used for the parameter identification using PSO.

As in the previous case, the discharge region is of importance. Hence, the parameter particle trajectories are provided in Fig. 5(a)-(d), which shows only for the discharge region current. Here also, the particles each of the parameters converged to a single location from their initial positions. Such convergence provided the basis for the algorithm's superior performance in this case of battery parameter identification.

The fitness function for 24-hr over-discharged battery, which represents the global optimum value, is provided in Fig. 5(e). The identified parameters for this battery condition is provided in Table 5.

6.4. Over-charged battery parameter identification

The overcharged battery was attained using the following procedure. The discharge operation was carried out at 3.4 A (1 C) and the charge operation was carried out at 4.25 A (25% overcharge). This cycle was repeated for twenty (20) times.

Parameter identification was performed using the charging region of the last cycle since the charging region is critical for this battery condition. The particle positon update histories for each of the selected parameters for charging regime of operation is provided in Fig. 6(a)-(d).

The fitness function trajectory for this over-charged battery operation is provided Fig. 6(e). Observing the fitness function plot, it is clear that the objective function has been optimized. The identified parameters for this battery condition are provided in Table 6.

The cost or fitness function is same for all stated operating conditions of the battery. However, the convergence of the cost function depends on the initialization of the corresponding parameters. The convergence characteristics were similar in Figs. 3(e), 5(e) and 6(e). The converged value was checked in several more iterations to ensure that convergence was not premature. The convergence trend shown in Figs. 3–6 is very similar to that of the

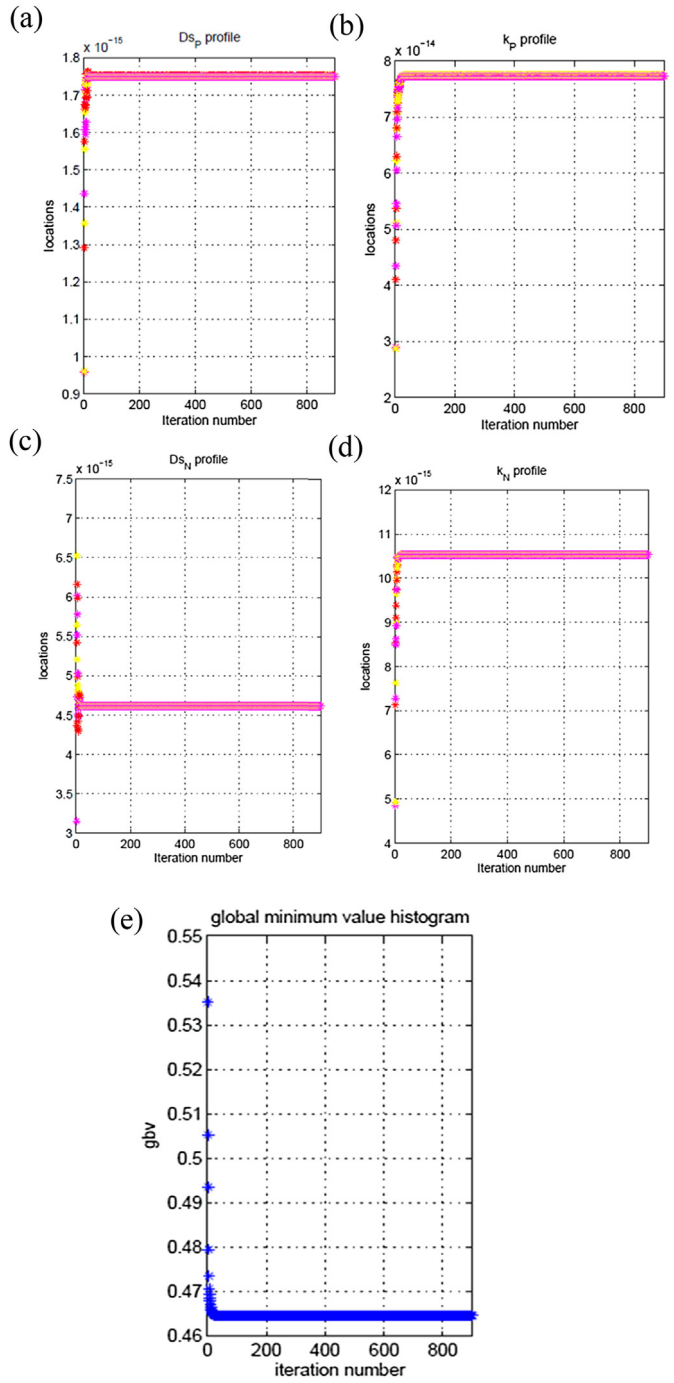

Fig. 3. (a)-(d)Particle update history of the healthy battery parameters (Charge operation); (e) Fitness function trajectory for healthy battery charge operation.

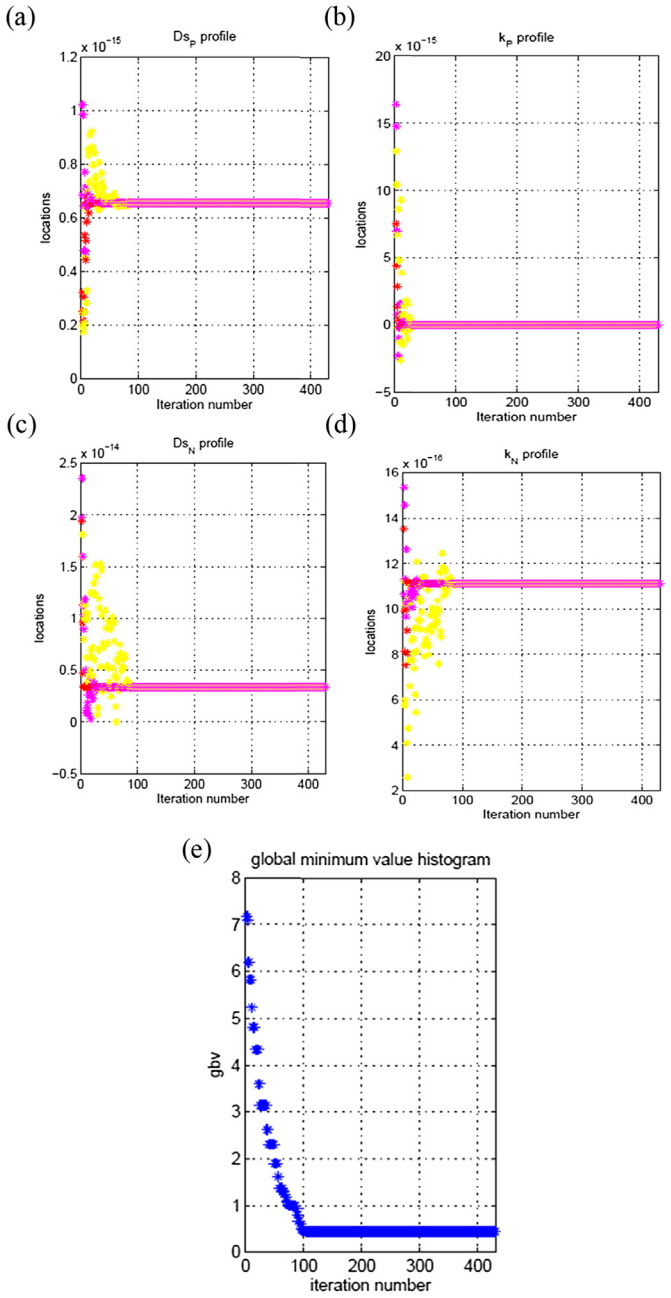

Fig. 4. (a)–(d) Particle update history of the Navy over-discharged battery parameters (Discharge operation); (e) Fitness function trajectory for Navy over-discharged battery discharge operation.

work reported in Ref. [33] which also shows very quick convergence of the fitness function using PSO algorithm in identifying model parameters.

Table 3
Identified items for healthy battery.

Identified item	For discharge	For charge
$D_{s,p}$	4.0264×10^{-16}	1.7507×10^{-15}
$D_{s,n}$	4.3196×10^{-14}	4.6174×10^{-15}
κ_p	6.0555×10^{-14}	7.7358×10^{-14}
κ_n	3.5484×10^{-15}	1.0532×10^{-14}
Optimum value of fitness function	0.4633	0.46458

Table 4
Identified items for Navy-OD battery.

Identified item	For discharge	For charge
$D_{s,p}$	6.5481×10^{-16}	2.0828×10^{-15}
$D_{s,n}$	3.35×10^{-15}	9.3458×10^{-16}
κ_p	7.3194×10^{-13}	5.4301×10^{-14}
κ_n	1.1129×10^{-15}	8.4599×10^{-15}
Optimum value of fitness function	0.4444	0.4577

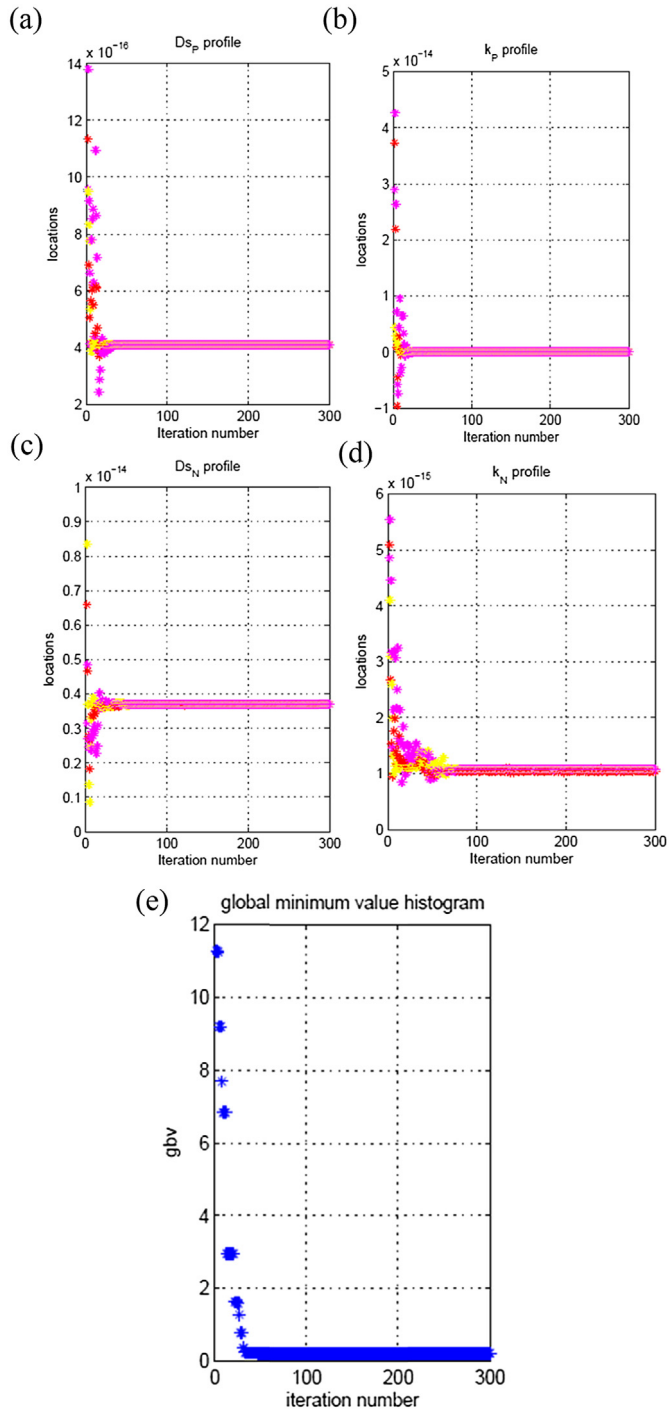

Fig. 5. (a)–(d) Particle update history of the 24 hr over-discharged battery parameters (Discharge operation); (e) Fitness function trajectory for 24 hr over-discharged battery discharge operation.

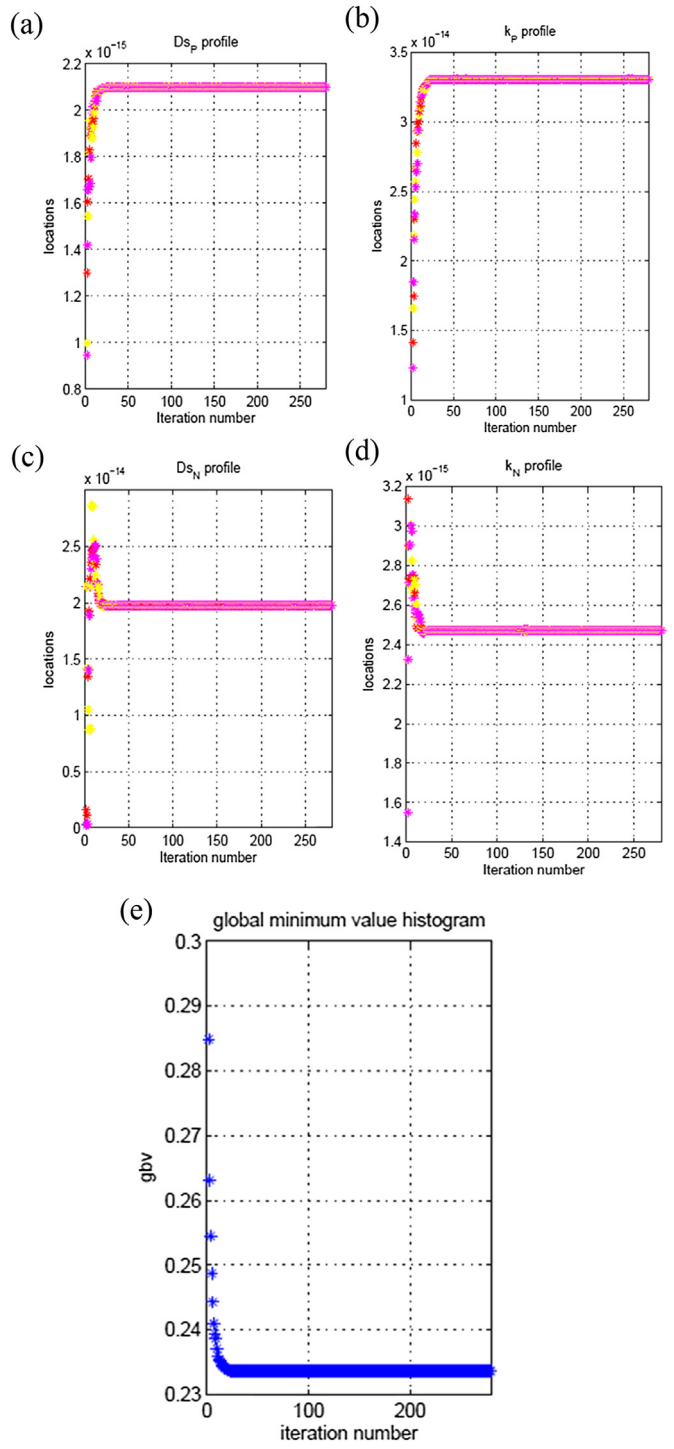

Fig. 6. (a)–(d) Particle update history of the over-charged battery parameters (Charge operation); (e) Fitness function trajectory for over-charged battery charge operation.

Table 5
Identified items for 24hr-OD battery.

Identified item	For discharge	For charge
$D_{s,p}$	4.0995×10^{-16}	1.8848×10^{-15}
$D_{s,n}$	3.6899×10^{-15}	9.5869×10^{-15}
κ_p	2.1611×10^{-13}	5.0345×10^{-14}
κ_n	1.0775×10^{-15}	3.3563×10^{-15}
Optimum value of fitness function	0.18081	0.17409

Table 6
Identified items for OC battery.

Identified item	For discharge	For charge
$D_{s,p}$	1.2884×10^{-16}	2.0986×10^{-15}
$D_{s,n}$	9.7622×10^{-15}	1.9827×10^{-14}
κ_p	3.3685×10^{-13}	3.3064×10^{-14}
κ_n	1.9175×10^{-15}	2.4734×10^{-15}
Optimum value of fitness function	0.23166	0.23364

7. Temperature variation

In the reduced electrochemical model of Li-Ion battery, the temperature was assumed to be constant at room temperature, namely 298.15 K. To check the validity of our assumption on temperature variation, the temperature was measured during the experiments.

Temperature variation during the experiments on the healthy battery is provided in Fig. 7(a). An analysis of the temperature profile reveals that the temperature changes only from 23° *C* to 24° *C* throughout the time of operation, i.e. only 1 °C variation, which is not significant enough to significantly influence the battery dynamics.

Temperature variation during the experiment for the Navy over-discharged battery (25% over-discharge) is provided in Fig. 7(b). Here, temperature changes from 24° °*C* to 25° *C* which is only 1 °C variation in temperature during this over-discharged experiment.

Similarly, the temperature variation during experiments on another over-discharged battery, namely the 24hr over-discharged battery (20% over-discharge) is provided in Fig. 7(c). Here also, temperature changes from 22° °*C* to 23° *C*, i.e. only 1° *C* variation, which is consistent with the assumption.

Temperature variation during the overcharging (25% over-charge) battery operation is provided in Fig. 7(d). During this operating condition, temperature changes only one degree, i.e. 23° *C* to 24° *C*.

Therefore, overall the temperature variation during the four experimental scenarios was very small and thus the validity of the assumption on temperature in the electrochemical modeling of Li-Ion battery dynamics holds.

8. Model validation

To validate the reduced order electrochemical model of the Li-Ion battery with the identified parameters, experimental voltage response was compared with the model predicted voltage response, which utilizes the identified electrochemical battery parameters (through the PSO algorithm). In this section, the voltage comparisons for different operating conditions (or the battery states) are provided.

To validate the electrochemical model with the identified parameters for healthy battery, the previously conditioned battery (healthy state) was taken under test and was cycled only once. The discharge (1 C) and charge (1 C) current data was used as the input to the battery model to compare with the relevant experimental voltage response. For discharge at 3.4 A current, the model output voltage and the experimentally measured voltage are compared and are shown in Fig. 8(a). Similar comparison was performed for the healthy battery with the stated charging current as the model input and the comparison of the respective voltage responses is provided in Fig. 8(b). From the comparison of voltages for both discharge and charge operation of the battery, it is clear that the identified battery parameters (through PSO algorithm) provides an accurate validation of the reduced electrochemical model of Li-Ion battery.

To validate the Navy over-discharged battery electrochemical

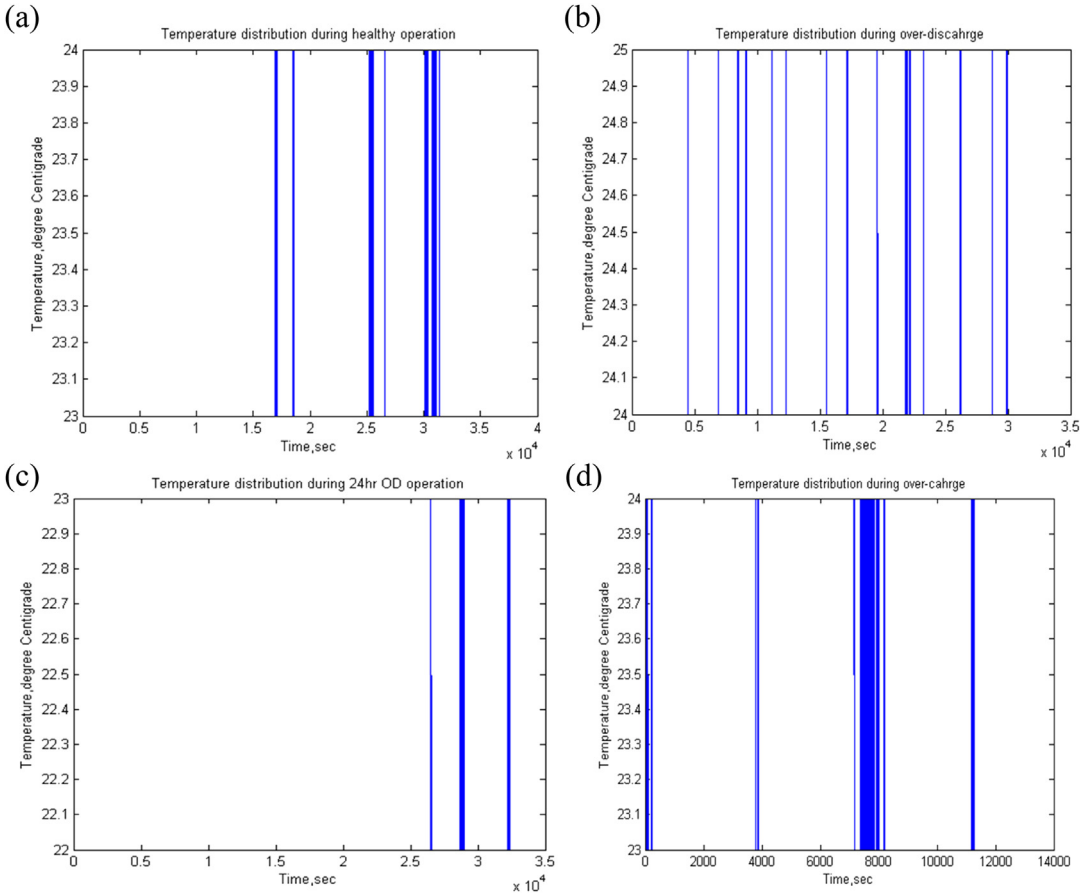

Fig. 7. (a) Temperature variation during Healthy battery operation; (b) Temperature variation during Navy over-discharge operation; (c) Temperature variation during 24 hr over-discharge operation; (d) Temperature variation during over-charge operation.

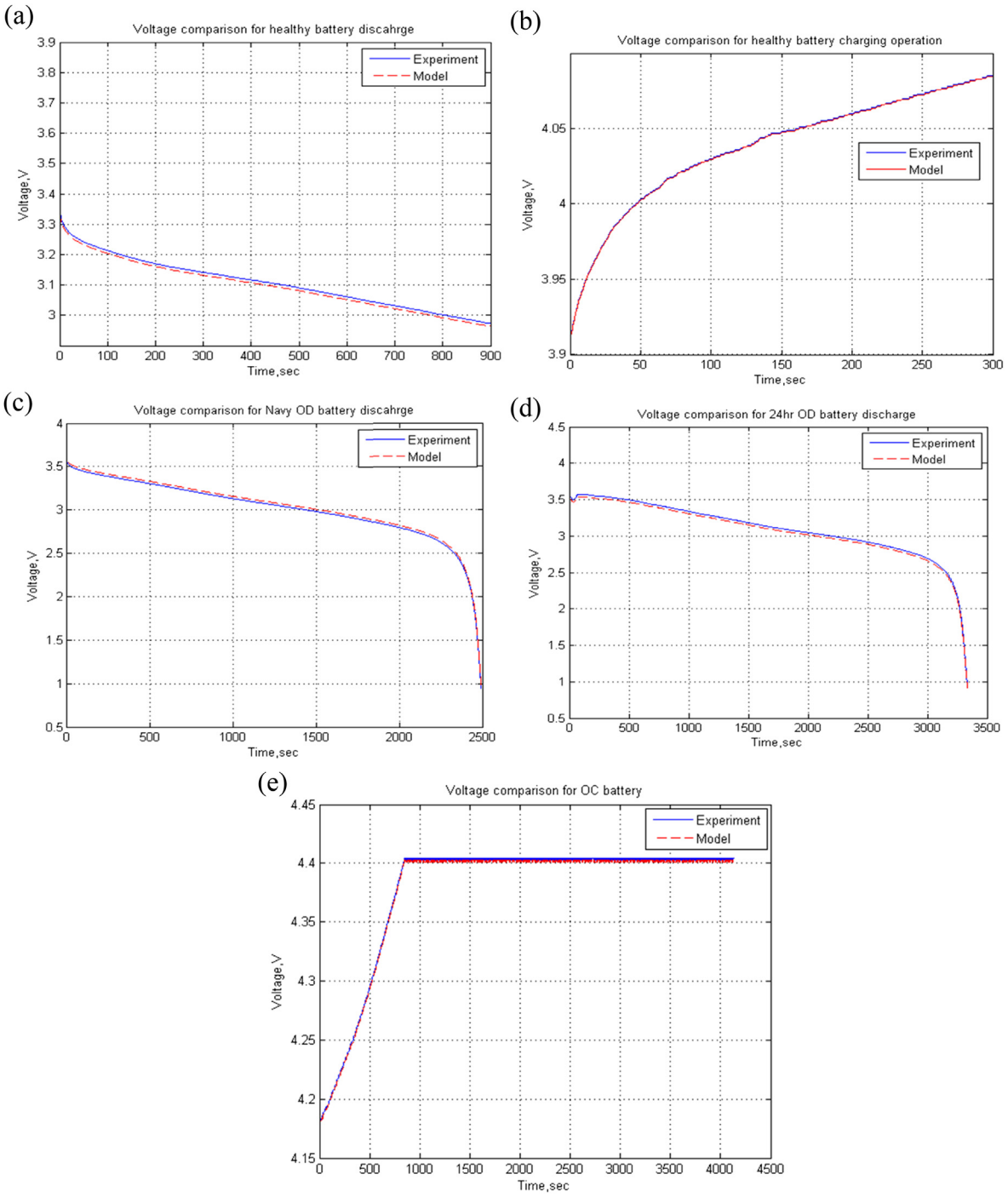

Fig. 8. (a) Voltage comparison for healthy battery discharge operation; (b) Voltage comparison for healthy battery charge operation; (c) Voltage comparison for Navy over-discharged battery discharge operation; (d) Voltage comparison for 24 hr over-discharged battery discharge operation; (e) Voltage comparison for overcharged battery charge operation.

model using the PSO identified parameters, the conditioned battery was again considered for test in a similar manner but at different rate of over-discharge. For parameter identification purpose, the battery was 25% over-discharged (1.25 C). But for model validation purpose, the battery was over-discharged at 15% (1.15 C) while the charge of the battery was carried out at normal rate (1 C). This cycle was performed only once. As the discharge operation of this battery is of significance here than the charge operation, the model validation is performed for only the discharge operation for the identified parameters. The model and experimental output voltage are compared in Fig. 8(c). From the voltage comparison for the discharge operation of the Navy OD battery, it is evident that the PSO identified battery parameters for this battery state or condition offers an accurate battery model.

For the 24-hr over-discharged battery model validation, previously conditioned battery at 1.2 C discharge (20% over-discharged) was taken under test for one cycle at different rate of over-discharge. For validation purpose, the battery was 10% over-

discharged (1.1 C), while the charging operation was maintained at the nominal rate (1 C). As in the case for the Navy over-discharged battery, the voltage comparison for only the discharge operation is performed for the model validation purpose for this case as well. The model and experimental output voltages are shown in Fig. 8(d). It is clear from this figure that the PSO identified parameters of the electrochemical model for the 24-hr over-discharged battery is accurate.

Lastly, the model validation of the over-charged battery is performed. Here the previously conditioned battery at 25% over-charge (1.25 C) operation was taken under test for one cycle at 15% over-charge (1.15 C), while the discharge operation was carried out at 1 C rate as before. The charging profile is shown in Fig. 8(e). From the voltage comparison of the over-charged battery model, it is clear that the battery model of the over-charged battery using the PSO identified parameters is accurate as well.

9. Conclusion

Particle Swarm Optimization method was used to identify significant parameter variations presented in electrochemical model of a $LiCoO_2$ battery while experiencing various operating conditions such as healthy battery, Navy over-discharged battery, 24-h over-discharged battery, and overcharged battery. Experimentally recorded data was utilized to validate the reduced electrochemical model of the battery. It was observed that the optimal values of the fitness function for all four battery operating conditions were reached quickly. This is evidenced by the convergence characteristics, confirming the accuracy of the identified parameters. The identified battery model parameters offer four different battery electrochemical models based on the battery operating conditions, providing a basis for electrochemical model based condition monitoring.

References

[1] R. Klein, N.A. Chaturvedi, J. Christensen, J. Ahmed, R. Findeisen, A. Kojic, Electrochemical model based observer design for a lithium-ion battery, Control Syst. Technol. IEEE Trans. 21 (2013) 289–301.

[2] J.-M. Tarascon, M. Armand, Issues and challenges facing rechargeable lithium batteries, Nature 414 (2001) 359–367.

[3] N.A. Chaturvedi, R. Klein, J. Christensen, J. Ahmed, A. Kojic, Modeling, estimation, and control challenges for lithium-ion batteries, in: American Control Conference (ACC), 2010, 2010, pp. 1997–2002.

[4] V. Wouk, Hybrid Electric Vehicles 277, Scientific American-American Edition, 1997, pp. 70–74.

[5] R. Poli, J. Kennedy, T. Blackwell, Particle swarm optimization, Swarm Intell. 1 (2007) 33–57.

[6] M. Clerc, J. Kennedy, The particle swarm-explosion, stability, and convergence in a multidimensional complex space, in: Evolutionary Computation, IEEE Transactions on 6, 2002, pp. 58–73.

[7] N. Chakraborti, R. Jayakanth, S. Das, E. Çalişir, Ş. Erkoç, Evolutionary and genetic algorithms applied to Li+-C system: calculations using differential evolution and particle swarm algorithm, J. Phase Equilibria Diffusion 28 (2007) 140–149.

[8] N. Chakraborti, S. Das, R. Jayakanth, R. Pekoz, Ş. Erkoç, Genetic algorithms applied to Li+ ions contained in carbon nanotubes: An investigation using particle swarm optimization and differential evolution along with molecular dynamics, Mater. Manuf. Process 22 (2007) 562–569.

[9] J.C. Forman, S.J. Moura, J.L. Stein, H.K. Fathy, Genetic parameter identification of the Doyle-Fuller-Newman model from experimental cycling of a LiFePO 4 battery, in: American Control Conference (ACC), 2011, 2011, pp. 362–369.

[10] J.C. Forman, S.J. Moura, J.L. Stein, H.K. Fathy, Genetic identification and fisher identifiability analysis of the Doyle–Fuller–Newman model from experimental cycling of a LiFePO 4 cell, J. Power Sources 210 (2012) 263–275.

[11] Ahmed R., El Sayed M., Arasaratnam I., Tjong J., and Habibi S., "Reduced-Order Electrochemical Model Parameters Identification and SOC Estimation for Healthy and Aged Li-Ion Batteries. Part I: Parameterization Model Development for Healthy Batteries".

[12] N. Kwok, Q. Ha, T. Nguyen, J. Li, B. Samali, A novel hysteretic model for magnetorheological fluid dampers and parameter identification using particle swarm optimization, Sensors Actuators A Phys. 132 (2006) 441–451.

[13] V. Ramadesigan, V. Boovaragavan, M. Arabandi, K. Chen, H. Tsukamoto, R. Braatz, et al., Parameter estimation and capacity fade analysis of lithium-ion batteries using first-principles-based efficient reformulated models, ECS Trans. 19 (2009) 11–19.

[14] V.R. Subramanian, V. Boovaragavan, V.D. Diwakar, Toward real-time simulation of physics based lithium-ion battery models, Electrochem. Solid-State Lett. 10 (2007) A255–A260.

[15] C. Speltino, D. Domenico, G. Fiengo, A. Stefanopoulou, Experimental identification and validation of an electrochemical model of a lithium-ion battery, in: Proceedings of the American Control Conference, 2009.

[16] M. Doyle, T.F. Fuller, J. Newman, Modeling of galvanostatic charge and discharge of the lithium/polymer/insertion cell, J. Electrochem. Soc. 140 (1993) 1526–1533.

[17] J. Newman, W. Tiedemann, Porous-electrode theory with battery applications, AIChE J. 21 (1975) 25–41.

[18] K.A. Smith, C.D. Rahn, C.-Y. Wang, Control oriented 1D electrochemical model of lithium ion battery, Energy Convers. Manag. 48 (2007) 2565–2578.

[19] N.A. Chaturvedi, R. Klein, J. Christensen, J. Ahmed, A. Kojic, Algorithms for advanced battery-management systems, Control Syst. IEEE 30 (2010) 49–68.

[20] R. Klein, N.A. Chaturvedi, J. Christensen, J. Ahmed, R. Findeisen, A. Kojic, State estimation of a reduced electrochemical model of a lithium-ion battery, in: American Control Conference (ACC), 2010, 2010, pp. 6618–6623.

[21] P. Albertus, J. Christensen, J. Newman, Experiments on and modeling of positive electrodes with multiple active materials for lithium-ion batteries, J. Electrochem. Soc. 156 (2009) A606–A618.

[22] V.R. Subramanian, V. Boovaragavan, V. Ramadesigan, M. Arabandi, Mathematical model reformulation for lithium-ion battery simulations: Galvanostatic boundary conditions, J. Electrochem. Soc. 156 (2009) A260–A271.

[23] V.R. Subramanian, V.D. Diwakar, D. Tapriyal, Efficient macro-micro scale coupled modeling of batteries, J. Electrochem. Soc. 152 (2005) A2002–A2008.

[24] J. Vesterstrom, R. Thomsen, A comparative study of differential evolution, particle swarm optimization, and evolutionary algorithms on numerical benchmark problems, in: Evolutionary Computation, 2004. CEC2004. Congress on, 2004, pp. 1980–1987.

[25] Q. He, L. Wang, B. Liu, Parameter Estimation for Chaotic Systems by Particle Swarm Optimization Chaos, Solitons & Fractals 34, 2007, pp. 654–661.

[26] H. Modares, A. Alfi, M.-M. Fateh, Parameter identification of chaotic dynamic systems through an improved particle swarm optimization, in: Expert Systems with Applications 37, 2010, pp. 3714–3720.

[27] C.-M. Huang, C.-J. Huang, M.-L. Wang, A particle swarm optimization to identifying the ARMAX model for short-term load forecasting, in: Power Systems, IEEE Transactions on 20, 2005, pp. 1126–1133.

[28] R.C. Eberhart, Y. Shi, Particle swarm optimization: developments, applications and resources, in: Evolutionary Computation, 2001. Proceedings of the 2001 Congress on, 2001, pp. 81–86.

[29] K.E. Parsopoulos, M.N. Vrahatis, Recent approaches to global optimization problems through particle swarm optimization, Nat. Comput. 1 (2002) 235–306.

[30] R.C. Eberhart, J. Kennedy, A new optimizer using particle swarm theory, in: Proceedings of the Sixth International Symposium on Micro Machine and Human Science, 1995, pp. 39–43.

[31] G. Venter, J. Sobieszczanski-Sobieski, Particle swarm optimization, AIAA J. 41 (2003) 1583–1589.

[32] V.K. Muddappa, S. Anwar, Electrochemical model based fault diagnosis of Li-ion battery using Fuzzy Logic, in: ASME 2014 International Mechanical Engineering Congress and Exposition, 2014 pp. V04BT04A048–V04BT04A048.

[33] P. Manoharan, P. Kannan, S. Baskar, M.W. Iruthayarajan, Evolutionary algorithm solution and KKT based optimality verification to multi-area economic dispatch, Int. J. Electr. Power Energy Syst. 31 (2009) 365–373.